

# DETERMINATION OF BULK AND SURFACE SUPERCONDUCTING PROPERTIES OF N<sub>2</sub>-DOPED COLD WORKED, HEAT TREATED AND ELECTRO-POLISHED SRF GRADE NIOBIUM

S. Chetri, D.C. Larbalestier, P.J. Lee, Applied Superconductivity Center,  
National High Magnetic Field Laboratory, FSU, FL 32310, USA

P. Dhakal, Thomas Jefferson National Accelerator Facility, VA 23606, USA

Z-H Sung, United States Steel Research and Technology Center, PA 15120, USA

## Abstract

Nitrogen-doped cavities show significant performance improvement ( $Q_0$ ) beyond the expected limits due to lowered RF surface resistance [1,2]. However, such cavities quench in the medium accelerating field regime ( $B_{peak} = 80 - 120$  mT) for reasons that remain to be clearly explained. In this study we explore the influence of N<sub>2</sub>-doping on the surface and bulk superconducting properties of cold worked SRF Nb, and then compare these results with those previously obtained on similarly cold worked samples given conventional cavity processing without N<sub>2</sub> treatments. We present DC magnetization and AC susceptibility characteristics of a polycrystalline Nb rod drawn to a true strain of 4.2, after standard cavity chemical, thermal, and N<sub>2</sub>-doping treatments. DC magnetic hysteresis showed that the N<sub>2</sub>-doping significantly decreases the field of first flux penetration,  $H_{cp}$ . Temperature-variation-mode AC susceptibility showed that N<sub>2</sub>-doping after an 800°C anneal enhances the surface critical temperature,  $T_{c,onset} \sim 9.4$  K to values similar to that observed for 120°C baking, suggestive of strong surface charging by nitrogen. Use of DC as well as AC techniques allows us to see that the bulk  $T_{c,peak}$  shifts back to the typical  $T_c$  of annealed Nb,  $\sim 9.2$  K after 800°C, even as  $T_{c,onset}$  is enhanced by N<sub>2</sub>. It is also observed that  $r_{32}$  ( $H_{c3}/H_{c2}$ ) ratio reverts to the Ginzburg-Landau (GL) value of  $\sim 1.7$ . The implication is clearly that N<sub>2</sub>-doping affects the surface superconductivity of SRF-Nb without deteriorating the bulk properties.

## INTRODUCTION

Recently, a nitrogen doping step has been introduced into the processing of SRF cavities which has resulted in an enhanced quality factor ( $Q_0$ ) beyond the previously assumed theoretical limits [1]-[2]. However, this enhanced performance is offset by quenching in the mid RF field regime ( $B_{peak} \approx 80 - 120$  mT) [2]. The mid field quench phenomenon of the N<sub>2</sub>-doped cavity appears near the lower critical field of niobium, thus implicating vortex penetration as its cause. Measurement of  $H_{cp}$ , the field of first flux penetration and its relationship to the often enhanced surface superconductivity critical field,  $H_{c3}$ , thus seems important. Our previous study of SRF-grade polycrystalline Nb [3] by surface-sensitive AC susceptibility showed that cold work can enhance the surface superconducting properties ( $T_{c,onset}$  and the  $r_{32}$  ( $H_{c3}/H_{c2}$ ) ratio), an observation that is in agreement with

Casalbuoni's earlier study which showed that standard chemical and thermal cavity treatments enhance the surface superconductivity well beyond the GL ratio of  $\sim 1.7$  [4]. Following our previous study, here we have investigated the surface and bulk superconductivity of Nb samples given the same processing history as the earlier samples, but with an additional recrystallization at 800°C and N<sub>2</sub>-doping step as recently employed in cavity fabrication. To characterize variations of surface and bulk superconductivity, we combined AC susceptibility with DC magnetic hysteresis. We are also implementing X-ray Photoelectron Spectroscopy (XPS), surface chemistry analysis in order to provide additional interpretation of the current findings.

## EXPERIMENTAL

A SRF-grade poly-crystalline Nb rod was drawn to a true strain of 4.2, and then processed using the standard SRF Nb cavity fabrication steps established for the ILC (international linear collider): EP (electro-polishing), BCP (buffered chemical polishing), 120°C/48h bake, and 800°C/2h anneal. Our previous study [3] employing these processing steps showed a strong relationship between surface superconductivity and mechanical deformation. In order to clarify the new effects of N<sub>2</sub>-doping, several sets of these drawn Nb samples were sent to Thomas Jefferson National Accelerator Facility (TJNAF) for recrystallization and nitrogen doping. These samples were in the as-drawn, 3h EP'ed and 95min BCP'ed condition, with diameter (0.75-1 mm).

These Nb rods were first annealed at 800°C for 3 h in a chamber used for cavity heat treatments and at the end of the anneal nitrogen gas was injected into the furnace at a partial pressure of  $\sim 25$  mTorr for 2 minutes after which the N<sub>2</sub> was removed and a final anneal at 800°C for 10 minutes was given in order to diffuse N into the bulk. After return to room temperature, the N<sub>2</sub>-doped samples were further treated with an extra 10 min EP that removed  $\sim 5$   $\mu$ m of surface to follow the previous practice established for N<sub>2</sub>-doped cavity processing.

After the doping process, the Nb wires were cut into  $\sim 7$  mm lengths with a diamond saw in order to fit into the cryostat of the surface and bulk superconducting property measurement system. AC susceptibility was characterized in DC field-swept and temperature-variation mode with a 9 T Quantum Design PPMS (Physical Property Measurement System). Since the relevant layer for SRF performance is that within a penetration depth of the

surface ( $\lambda(\text{Nb}) \sim 40\text{-}50$  nm), we applied an AC field of amplitude  $10 \mu\text{T}$  and frequency  $100$  Hz to probe the surface properties to this depth. We determined  $T_{c,\text{onset}}$  as the first deviation from the normal conducting state and  $T_{c,\text{peak}}$  is defined by the main peak in the imaginary part  $\chi''$  of the complex AC susceptibility  $\chi(T) = \chi'(T) + i\chi''(T)$ . Bulk properties were derived from DC magnetization performed in a 5 T Quantum Design SQUID (Superconducting Quantum Interference Device) system. During these DC and AC measurements, the rod samples were aligned parallel to the external magnetic field as would be the case for RF cavity operation. The cylindrical shape of the rods minimizes the demagnetization effect on the magnetization measurements.

## RESULTS

### Critical Temperature

Figure 1 shows the surface-sensitive AC susceptibilities (imaginary part,  $\chi''$ ) of the 3 h EP'ed and 95 min BCP'ed Nb wires after different cavity treatments ( $120^\circ\text{C}/48\text{h}$  bake,  $800^\circ\text{C}/2\text{h}$  anneal,  $\text{N}_2$ -doping at  $800^\circ\text{C}/3\text{h}$ , and  $\text{N}_2$ -doping with an extra 10 min EP) measured at 2 mT applied field.

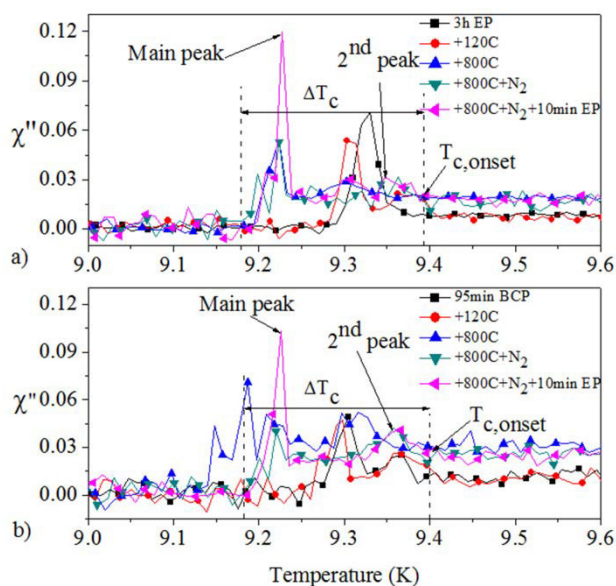


Figure 1: Temperature-variation-mode of AC susceptibilities (imaginary,  $\chi''$ ), on 3 h EP'ed (a) and 95 min BCP'ed (b) Nb wires at  $10 \mu\text{T}$  and  $100\text{Hz}$  as a function of surface treatment.

In nitrogen-doped Nb wires,  $T_{c,\text{onset}}$  appears near  $\sim 9.4$  K with the secondary peak at  $\sim 9.36$  K, results very similar to those shown for the  $120^\circ\text{C}/48\text{h}$  baked wire and slightly higher than for the  $800^\circ\text{C}/2\text{h}$  annealed wire. However,  $T_{c,\text{peak}}$ , characteristic of the bulk properties shifts towards the expected value of  $\sim 9.2$  K for pure Nb with  $\text{N}_2$ -doping process. Compared to the 3 h EP'ed wires, the 95 min

BCP'ed wires show a higher noise ratio. However, these BCP'ed wires also have enhanced  $T_{c,\text{onset}}$  with the secondary peak and  $T_{c,\text{peak}}$  shifted back to  $\sim 9.2$  K after the  $\text{N}_2$ -doping process. The  $T_{c,\text{onset}}$ ,  $T_{c,\text{peak}}$ , the secondary peak, and  $\Delta T_c$  are tabulated in Table 1 for all the samples. It is found that  $\text{N}_2$ -doping increases  $T_{c,\text{onset}}$  close to the value for the  $120^\circ\text{C}$  bake regardless of the surface chemical treatment employed even as, presumably, the  $800^\circ\text{C}$  anneal shifts  $T_{c,\text{peak}}$  back to  $\sim 9.2$  K. The  $\text{N}_2$ -doping process increases the transition width,  $\Delta T_c$  due to this enhancement of the difference between surface and bulk properties. The table also shows that there is no significant change in  $T_{c,\text{peak}}$  after the extra 10 min EP (which removes  $\sim 5 \mu\text{m}$  of outer surface, i.e.  $\gg$  penetration depth). However, there is a slight increase in the  $T_{c,\text{onset}}$ , hinting that the extra EP introduced some impurities into the surface.

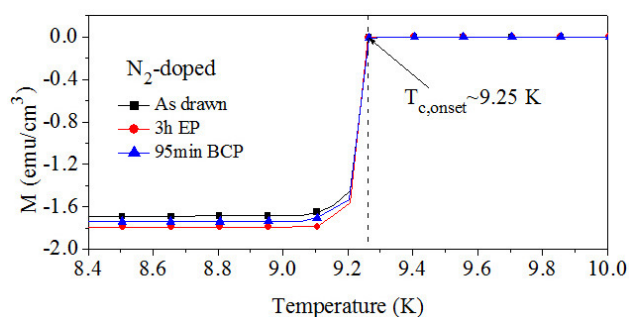


Figure 2: Temperature-swept DC magnetization curve of the  $\text{N}_2$ -doped Nb from SQUID characterization at 2 mT applied field.

Figure 2 shows bulk-dominated, DC magnetization hysteresis curve evaluated using the SQUID system. The bulk  $T_{c,\text{onset}}$  point indicated by the arrow occurs as expected for annealed Nb at  $\sim 9.25$  K and closely corresponds to  $T_{c,\text{peak}}$  (the primary peak) in the imaginary part of the AC susceptibility, indicating that our temperature-variation-mode AC susceptibility measurement can reveal both surface and bulk superconducting transitions in SRF-Nb.

Table 1: The onset of  $T_c$ , the primary peak ( $T_{c, peak}$ ), the secondary peak and the transition width ( $\Delta T_c$ ) of the as drawn, 3h EP'ed and 95min BCP'ed wires with various treatment from temperature-variation-mode AC susceptibility characterization at 10  $\mu$ T and 100 Hz.

Sample type	$T_{c, onset}$	$T_{c, peak}$ (Main peak)	Secondary peak	$\Delta T_c$
As-drawn	9.46	9.34	-	0.15
As-drawn+120°C	9.43	9.31	9.40	0.15
As-drawn+800°C	9.39	9.18	9.35	0.23
As-drawn+800°C+N <sub>2</sub>	9.41	9.22	9.36	0.23
As-drawn+800°C+N <sub>2</sub> +10min EP	9.38	9.22	9.36	0.20
3h EP	9.38	9.33	-	0.09
3h EP+120°C	9.41	9.30	9.37	0.13
3h EP+800°C	9.34	9.23	9.30	0.15
3h EP+800°C+N <sub>2</sub>	9.39	9.22	9.36	0.24
3h EP+800°C+N <sub>2</sub> +10min EP	9.40	9.23	9.32	0.21
95 min BCP	9.38	9.31	9.33	0.10
95 min BCP+120°C	9.41	9.30	9.31	0.15
95 min BCP+800°C	9.35	9.19	9.31	0.21
95 min BCP+800°C+N <sub>2</sub>	9.39	9.22	9.36	0.21
95 min BCP+800°C+N <sub>2</sub> +10min EP	9.39	9.22	9.36	0.20

### Bulk Superconducting Properties

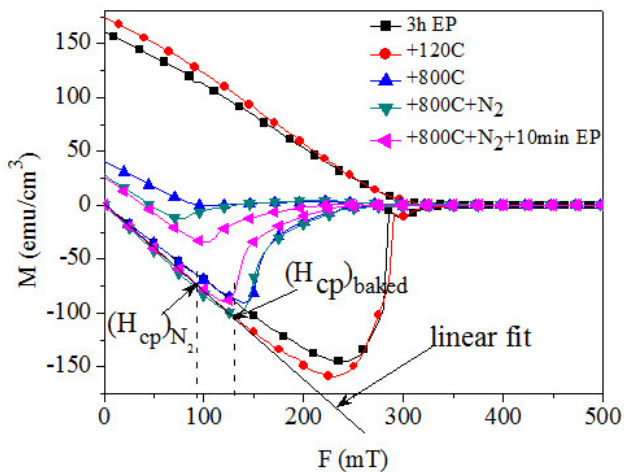


Figure 3: DC magnetic hysteresis curves of the 3h EP'ed Nb wire at 5 K with different surface treatments.

Bulk magnetic moments were measured by SQUID magnetometry with DC magnetic fields applied parallel to the Nb wire surface. As usual hysteresis due to surface barrier and vortex pinning makes it difficult to exactly determine  $H_{c1}$  due to the sensitivity of the surface to SRF treatments. Accordingly we define a simple characteristic by the first onset of magnetic flux penetration,  $H_{cp}$ , using the first deviation from a linear fit to the DC magnetization curve, as shown in Fig. 3. Figure 3 shows a DC magnetization curve for the 3h EP'ed Nb wire after

several different cavity treatments.  $H_{cp}$  significantly decreases after N<sub>2</sub>-doping and an additional 10 min EP process step. This trend is identical to that seen in the as-drawn and BCP'ed sample set (figures not presented for conciseness of paper). However, additional EP that removes more of the N<sub>2</sub>-influenced surface layer seems to have no influence on  $H_{cp}$  as shown in Fig. 4.

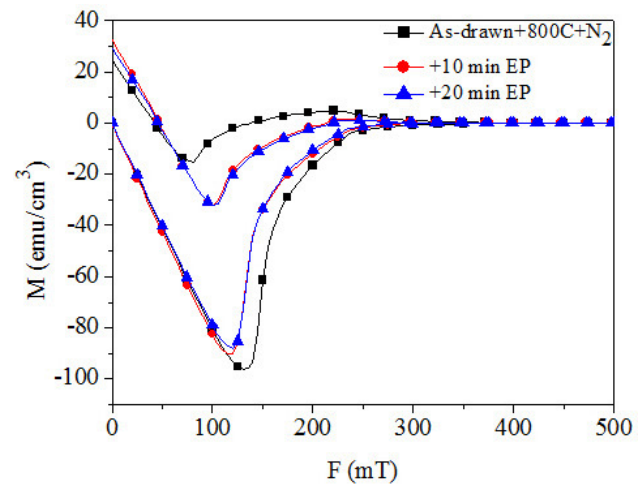


Figure 4: Comparison of DC magnetic hysteresis curves of N<sub>2</sub>-doped 95 min BCP'ed Nb wires at 5 K with varying EP process times.

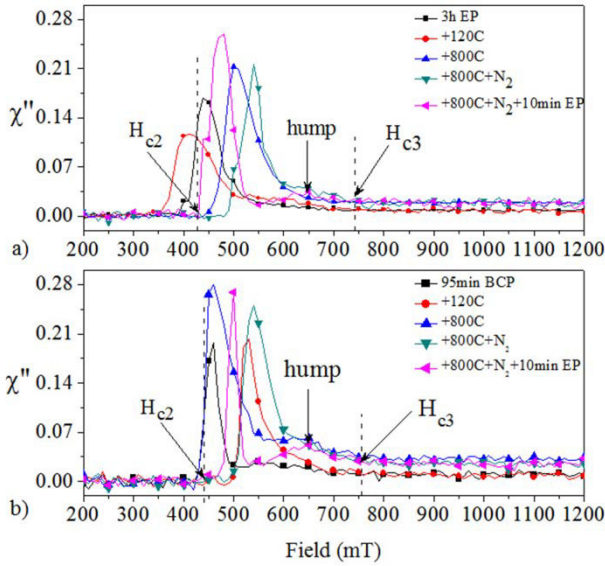


Figure 5: Imaginary part,  $\chi''$ , of DC magnetic field-swept-mode AC susceptibilities of (a) 3h EP and (b) 95min BCP'ed Nb with different surface treatments.

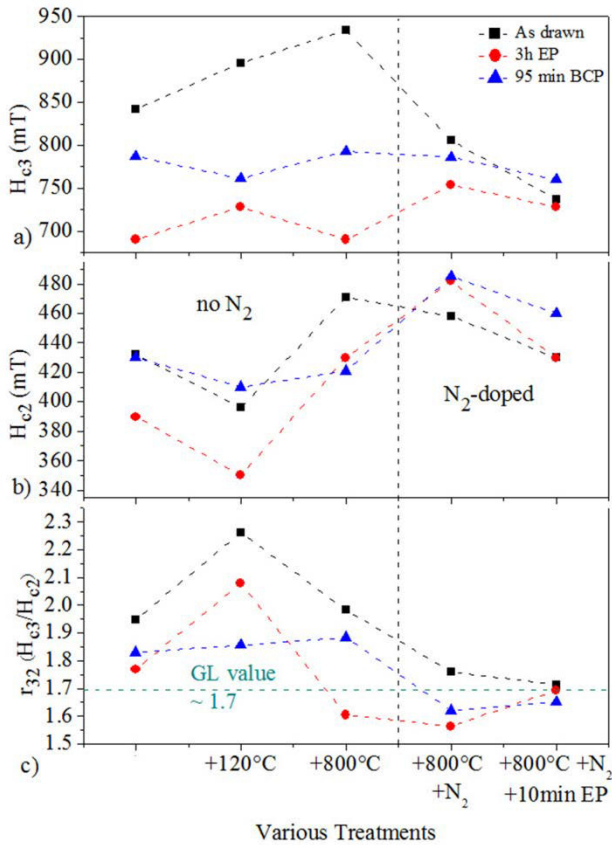


Figure 6: Variation of (a)  $H_{c3}$ , (b)  $H_{c2}$ , & (c)  $r_{32}$  ( $H_{c3}/H_{c2}$ ) ratio of all the samples tested with different cavity fabrication process based on DC magnetic-field-swept AC susceptibility.

### Surface Superconductivity

The nucleation of the superconducting phase in a thin surface sheath in a decreasing field was first discovered by Saint-James and de Gennes [5]. The surface critical field ( $H_{c3}$ ) and upper critical field ( $H_{c2}$ ) are determined from the imaginary part,  $\chi''$ , of the DC field-variation-mode AC susceptibility curves. The first deviation point from the normal conducting region in decreasing DC magnetic field defines  $H_{c3}$  and  $H_{c2}$  is determined by the onset field at which  $\chi''$  becomes zero.

Figure 5 shows the imaginary part of DC magnetic field-swept-mode AC susceptibility curves for 3h EP'ed and 95min BCP'ed Nb wires after various cavity treatments. A small hump appears just below  $H_{c3}$  on the  $N_2$  doped samples and becomes more dominant after the final 10 min EP.

Figure 6 compares the variation of  $H_{c3}$ ,  $H_{c2}$  and  $r_{32}$  ( $H_{c3}/H_{c2}$ ) ratio of all the samples tested. Among the chemically treated Nb wires there is no noticeable change in  $H_{c3}$  value, even after  $N_2$ -doping. But, in the case of As-drawn Nb wires,  $H_{c3}$  is reduced after  $N_2$ -doping. The  $H_{c2}$  value is increased for the  $N_2$ -doped samples, but is slightly reduced after additional EP. However, the  $r_{32}$  ( $H_{c3}/H_{c2}$ ) ratio drops close to ideal GL value of  $\sim 1.7$  after annealing and  $N_2$ -doping.

### DISCUSSION

Nitrogen doping of these cold worked niobium rods results in enhanced  $T_{c,onset}$  values. Unlike, low temperature baked Nb rods, this  $T_c$  enhancement for the  $N_2$ -doped Nb rods is close to the ideal value for bulk behaviour as evident from the main  $T_{c,peak}$  shifted towards the ideal value of  $\sim 9.2$  K value. The bulk  $T_c$  measurement using the SQUID also confirms this behaviour. This suggests that the  $N_2$ -doping process which occurs at the end of an  $800^\circ\text{C}/3\text{h}$  anneal) is aiding in the recovery of the highly deformed and inter-curved grains created by the wire-drawing that was shown in the previous EBSD-OIM micro-crystallographic analysis [3] on  $800^\circ\text{C}/2\text{h}$  annealed wires. If interstitial segregation to the grain boundaries in the earlier sample set inhibited the full recovery of the surface region then these results suggest that the  $N_2$  doping removes or modifies this interstitial segregation.

The appearance of the hump-like secondary peak in both the temperature-variation-mode and field-swept-mode AC susceptibility measurements indicates that the surface of  $N_2$ -doped Nb is getting dirty with additional constituents dissipating the surface current. It is likely that Nitrogen is interstitially present in the near surface Nb lattice.

The decrease in the flux pinning as indicated by the reduction in area under DC magnetization curve of  $N_2$ -doped wires could be explained by hydrogen being trapped by nitrogen and thus suppressing the formation of hydrides that might otherwise act as pinning centers. From the study presented in [6], nitrogen being

interstitially present has a tendency to trap hydrogen inhibiting the formation of hydrides and this could explain the measured reduction in residual resistance for N<sub>2</sub>-doping [2].

It is likely that N<sub>2</sub>-doping decreases  $H_{c3}$  of the as-drawn, suggesting that nitrogen may trap hydrogen atoms at cryogenic temperatures if “H” is the only impurity in the as-drawn wire. However, there is no significant N effect on  $H_{c3}$  of chemically treated Nb wires. On the other hand it is clear that N<sub>2</sub>-doping affects  $H_{c2}$ , resulting in significant drop of  $r_{32}$  ( $H_{c3}/H_{c2}$ ) ratio, close to GL  $\sim 1.7$ .

## CONCLUSION

We have investigated the changes in surface and bulk superconducting properties of cold worked SRF-Nb niobium after N<sub>2</sub>-doping treatment by applying AC susceptibility and DC magnetic hysteresis characterization. We found that the N<sub>2</sub>-doping process can enhance surface superconductivity, close to the level of the 120°C bake and appears to aid in the recovery and recrystallization of the cold-worked deformed structures that had previously been resistant to recovery without N<sub>2</sub> doping. These results suggest that nitrogen may interact with interstitial sergeants that had previously blocked full recovery. To clarify this surface superconducting analysis, we are performing surface chemistry and microstructural characterization using XPS and EBSD-OIM.

## ACKNOWLEDGMENT

The support for this work at FSU was from US DOE Award # DE-SC0009960 and the State of Florida. Additional support for the National High Magnetic Field Laboratory facilities is from the National Science Foundation: NSF-DMR-1157490.

## REFERENCES

- [1] A. Grassellino, A. Romanenko, D. Sergatskov, O. Melnychuk, Y. Trenikhina, A. Crawford, A. Rowe, M. Wong, T. Khabiboulline, and F. Barkov, *Supercond. Sci. Technol.* **26**, 102001 (2013).
- [2] P. Dhakal, G. Ciovati, P. Kneisel, and G. R. Myneni, *IEEE Transactions on Applied Superconductivity*, **25**, 350104 (2015).
- [3] Z.-H. Sung, A. Dzyuba, P. J. Lee, D. C. Larbalestier, and L. D. Cooley, *Supercond. Sci. Technol.* **28**, 075003 (2015).
- [4] S. Casalbuoni, E.-A. Knabbe, J. Koetzler, L. Lilje, L. von Sawilski, P. Schmueser, and B. Steffen, *Nucl. Instrum. Methods Phys. Res. Sect. Accel. Spectrometers Detect. Assoc. Equip.* **538**, 45 (2005).
- [5] D. Saint-James and P. G. Gennes, *Phys. Lett.* **7**, 306 (1963).
- [6] D. C. Ford, L. D. Cooley, and D. N. Seidman, *Supercond. Sci. Technol.* **26**, 105003 (2013).